BRIEF COMMUNICATION

Near-magnetic-axis Geometry of a Closely Quasi-Isodynamic Stellarator

M.I. Mikhailov [a], J. Nührenberg[b1], R. Zille [b]

[a] *Russian Research Centre "Kurchatov Institute", Moscow,Russia*

[b] *Max-Planck-Institut für Plasmaphysik, EURATOM Assoziation, Teilinstitut Greifswald, Wendelsteinstr. 1, 17491 Greifswald, Germany*

Abstract

It is shown that the condition of stationary second adiabatic invariant at the magnetic axis of a stellarator configuration can be satisfied to good accuracy for all reflected particles.

Introduction

In the course of the introduction of quasi-isodynamicity [1], qi, deeply to moderately deeply reflected particles trapped in one period of a stellarator were considered. Inclusion of all reflected particles led to configurations with poloidally closed contours of the magnetic field strength on magnetic surfaces [2]. An integrated physics optimization of such a configuration led to promising neoclassical and magnetohydrodynamic properties [3]. An analysis of the qi quality of this configuration near its magnetic axis was performed in [4] and showed that qi is qualitatively but not closely realized. Here, it is investigated whether the qi property to lowest order in the distance from the magnetic axis, i.e the stationarity of the second adiabatic invariants for all reflected particles, can be achieved more closely.

A two-stage procedure is adopted; first, this problem is investigated in terms of the structure of the magnetic field strength in magnetic coordinates near the magnetic axis; then the solution is substantiated by finding the associated lowest-order flux-surface geometry.

Procedure

For the type of configurations discussed here, with stellarator symmetry and poloidally closed contours of B, it is appropriate to interpret ι as the rotational transform per period and the toroidal magnetic coordinate ϕ normalized to 2π for one period; so the qi property is to be considered in $0 \le \phi \le \pi$ and restricts the Fourier components of the field strength in leading order (square root of the normalized toroidal flux s): $B = B_{\rm o}(\phi) + s^{\frac{1}{2}} B_1(\theta,\phi)$ with $B_1(\theta,\phi) = \sum b_n \cos(\theta - n\phi)$. In magnetic coordinates, the relevant equation [1, 5] reads [2]

$$0 = \cos\iota\phi \sum b_n \cos(n\phi) + \sin\iota\phi \sum b_n \sin(n\phi)\,. \qquad (1)$$

Obviously the equation does not have a smooth solution. With the convention that $\phi = 0$ correspond to the minimum of $B_{\rm o}(\phi)$ and $\phi = \pi$ to its maximum, the area

[1] Corresponding author

[2] A nonvanishing integration constant in [5] would only imply that an even function cannot be equal to an odd function.

around $\phi = 0$ determines the behavior of the deeply trapped particles, the area around $\phi = \pi$ the behavior of the barely trapped ones. If the plasma β is not very large, deeply trapped particles are most endangered to be lost by radial drift. Barely trapped/transitional particles can get lost through collisionless diffusion. So, it might be useful to select approximate solutions satisfying the equation near the extrema of B_o. This is done here and shown that the qi condition can be closely approximated with few first-order Fourier components of the field strength. The three equations for first-order accuracy (in the distances from the endpoints 0 and π) are $\sum b_n = 0; \sum(-1)^{|n|} b_n = 0; \sum(-1)^{|n|} n b_n = 0$. In addition, the derivative at $\phi = 0$ of the odd part of B along a field line is required to vanish, $\sum n b_n = 0$, to avoid an extra local minimum of B near $\phi = 0$.

So, since the problem is linear, for example for a seven-components model a two-dimensional minimization problem results for the square of the qi condition.

Finally and more laboriously, the associated flux-surface geometry is found by optimization of the shape of the boundary of zero - β MHD equilibria.

Results

Since toroidal configurations are considered and quasihelically symmetric configurations are excluded here, it appears natural to employ b_0 (representing the toroidal effect) for normalization: $b_0 = -1$. Figure 1a shows the result for the two-parameter minimization for the set of seven Fourier components $[\, b_n, |n| \leq 3 \,]$ and a prescribed value of ι. Shown are the two terms of the qi condition, eq. 1, and their sum which exhibits a cancellation of a factor of about 7 compared to a single term and about 10 compared to the dominant helical component b_1. Figure 1b shows the result of the four-parameter minimization which, additionally, uses the components b_5 and b_{-5} and leads to a cancellation of about one-and-a-half orders of magnitude.

Realization of such a spectrum of the first order ($s^{\frac{1}{2}}$) of the field strength in magnetic coordinates was obtained by optimization of a stellarator with $N = 5$ periods and aspect-ratio $A \approx 14$ with its boundary, in VMEC [6] given by $R(u,v) = \Sigma R_{mn} \cos(mu - nv)$ and $Z(u,v) = \Sigma Z_{mn} \sin(mu - nv)$, solely comprising $m = 0$ and $m = 1$ Fourier coefficients. The result is shown in Fig. 2a, b. Fourier coefficients of B_1 beyond $|n| = 7$ have not been used so that a small tail of Fourier coefficients of O(10^{-4}) of the field strength persists as, for example, indicative of a modular-coil ripple. Figure 3 shows contours of B on this magnetic surface and elucidates how quasi-isodynamicity is realized. Figure 4 shows flux surface cross-sections; the main overall geometrical characteristic features are that the magnetic axis is not nearly helical (see, eg., Fig. 13 of [3]) but exhibits a dominant vertical excursion and the turning rate of the cross-section with respect to the z-direction is largest around the position of smallest ellipticity of the cross-section.

Discussion

The computational evaluation of the contours of the second adiabatic invariant is seen in Fig. 5 in the neighborhood of the magnetic axis. Thus, the stagnation point behavior is verified; attainment of quasi-isodynamicity at finite aspect ratio is a subject of further work. Since the diamagnetic effect at finite β is of higher order in the distance from the magnetic axis than considered in eq.(1), O-point behavior cannot be expected but nevertheless occurs for intermediate reflected particles. A detailed

consideration of particle orbits is only meaningful if, beyond the result found here, further work shows that all contours of the second adiabatic invariant can be closed poloidally.

Appendix

In [4] the qi condition was related to the near-axis geometry with the help of Mercier's expansion and noted that, for the qi case, a cancellation of rapidly varying functions, the torsion of the magnetic axis and the rotation of the elliptical flux surface cross-section, occurred which is due to measuring this rotation against the rotation of the normal to the magnetic axis. Here, in view of the simplicity of Fig. 4, the qi condition is obtained from the near-axis VMEC output directly, namely the geometry of an inner flux tube given by $\Sigma R_{mn}\cos(mu-nv)$ and $\Sigma Z_{mn}\sin(mu-nv)$ with $m=0,1$ so that $m=0$ describes the center of the flux tube and $m=1$ its boundary.

The strength of the magnetic field near the magnetic axis in the direction of the normal $\vec{n}$ to the centre of the flux tube (which coincides with the magnetic axis in the present approximation) is expressed as $B\kappa\xi(u,v)$ where the curvature κ is obtained from the $m=0$ coefficients and the distance $\xi(u,v)$ from the $m=1$ coefficients as follows. These coefficients lead to four functions $r_c(v)=\Sigma R_{1n}\cos nv$, $r_s(v)=\Sigma R_{1n}\sin nv$, $z_s(v)=\Sigma Z_{1n}\cos nv$ and $z_c(v)=-\Sigma Z_{1n}\sin nv$. Then, $\xi(u,v)$ is given by the projection of the position vector onto $\vec{n}$, so that $\xi=\xi_c\cos u+\xi_s\sin u$ with $\xi_c=r_cn_r+z_cn_z$ and $\xi_s=r_sn_r+z_sn_z$, so that the functions κn_r and κn_z occur in the first-order field strength; these functions only contain second derivatives along the center of the flux tube and are smooth independently of whether the curvature is small. To obtain the condition for quasi-isodynamicity, $\kappa(v)\xi(u,v)$ is now expressed in magnetic Boozer coordinates θ and ϕ (see, e.g. [7]). To the order needed the transformation is given by (F_T' derivative of toroidal flux wrt. s, I total poloidal current bounded by the flux tube in one period, $g_{uv}=\partial_u\vec{r}\cdot\partial_v\vec{r}$ etc.)

$u=\theta-\iota\frac{\tilde{\chi}_0}{I}+\frac{\lambda_0}{F_T'}$; $v=\phi-\frac{\tilde{\chi}_0}{I}$, where $\tilde{\chi}_0$ is given by

$(d/dv)\tilde{\chi}_0=I(g_{vv0}/\sqrt{g}_0)\tilde{}/<g_{vv0}/\sqrt{g}_0>_v$, with $<...>_v$ the v-average and $\tilde{}$ the variation of $g_{vv0}/\sqrt{g}_0$. ι and λ_0 are obtained as follows: the condition of vanishing toroidal current (as appropriate for qi-configuration), $\oint B_u du=0$, leads to an equation for λ_0 and λ_1 from which λ_1 is eliminated with the help of the first order of the condition that the current density lie in magnetic surfaces, $\partial_vB_u-\partial_uB_v=0$; the result is

$(\frac{\frac{d}{dv}\lambda_0}{F_T'}-\iota)<g_{vv0}g_{uu2}-g_{uv1}^2)>_u=<g_{vv0}g_{uv2}-g_{vv1}g_{uv1}+\sqrt{g}_0g_{uv1}\partial_v\int\frac{g_{uv1}}{\sqrt{g}_0}du'>_u$,

where the subscripts $0,1$ and 2 indicate the orders with respect to $s^{\frac{1}{2}}$. This equation leads to a formula for ι in terms of the geometry of the flux tube by appropriately averaging over v and then to λ_0 by integrating over v.

The evaluation is seen in Fig. 6 and shows that a solution of the problem discussed in this work could have been obtained, too, by optimization of an analytically given thin flux tube (in VMEC coordinates), which, however, then would not have been imbedded in a finite-aspect-ratio configuration.

Acknowledgments

This work was supported in part by the Russian Federation Presidential Program for State Support of Leading Scientific Schools (grant no. NSh-4361.2012.2). The support

of Prof. P. Helander is gratefully acknowledged.

Figure captions

Fig. 1.(a) The two terms of the qi condition, eq. 1, for $\iota = 0.173$ and their sum as functions of ϕ between the minimum and Maximum of B_o for b_0 = -1, b_3 = -1.095, b_{-3} = 0.778; (b) same as (a), but for b_3 = -0.952, b_{-3} = 0.603, b_5 = -0.111, b_{-5} = -0.111.

Fig. 2. (a) Same as Fig. 1 but without normalization at about a fifth of the minor radius of the configuration shown in Fig. 3 without b_8, b_9, b_{11}, b_{12} which were not part of the optimization; (b) with these coefficients.

Fig. 3. Contours of the magnetic field strength at 1/5 of the minor radius of the VMEC equilibrium.

Fig. 4. Six flux surface cross-sections equally spaced in toroidal direction along half a period.

Fig. 5. Contours of the second adiabatic invariant for deeply (first) to shallowly (third) reflected particles. The radial coordinate is the normalized toroidal flux.

Fig. 6. Evaluation of the qi condition directly from the VMEC output.

References

[1] S. Gori, W. Lotz, J. Nührenberg, *Proc. Joint Varenna-Lausanne Int. Workshop on Theory of Fusion Plasmas* (Bologna: Editrice Compositori, 1996) p.335.

[2] M.I. Mikhailov, J. Nührenberg, W.A. Cooper et al, *Nuclear Fusion* **42** 2002 L23.

[3] A.A. Subbotin, C. Nührenberg, V.V. Nemov et al, *Nuclear Fusion* **46** (2006) 921.

[4] M.I. Mikhailov, C. Nührenberg, J. Nührenberg, V.D. Shafranov et al, *38rd EPS Conf. on Plasma Phys.*, Strasbourg 2011, ECA, Vol.35G, P-5.043 (2006); (http://epsppd.epl.ch/Strasbourg/pdf/P5_043.pdf).

[5] V.D. Shafranov, *Plasma Phys. Control. Fusion* **43** (2001) A1.

[6] S.P. Hirshman and D.K. Lee, Comp. Phys. Commun. **39** (1986) 161.

[7] J. Nührenberg and R. Zille, Proc. Joint Varenna-Lausanne Int. Workshop on Theory of Fusion Plasmas (Varenna 1987)(Bologna: Editrice Compositori, 1988) p.3.

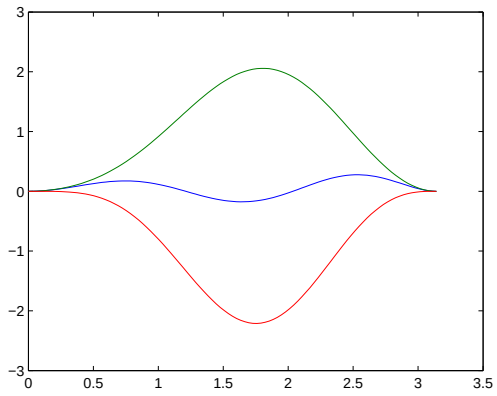

Figure 1a

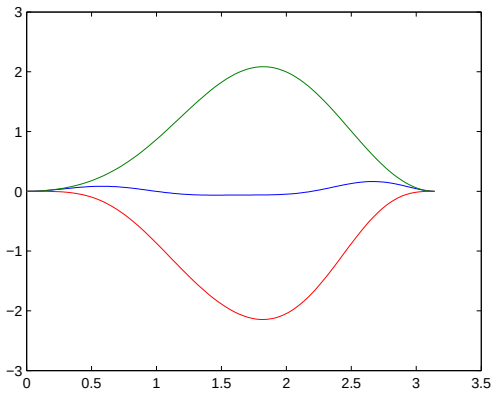

Figure 1b

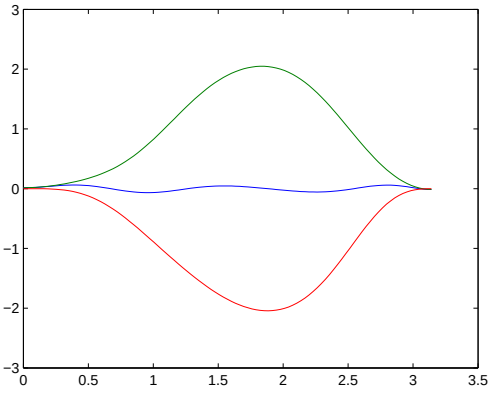

Figure 2a

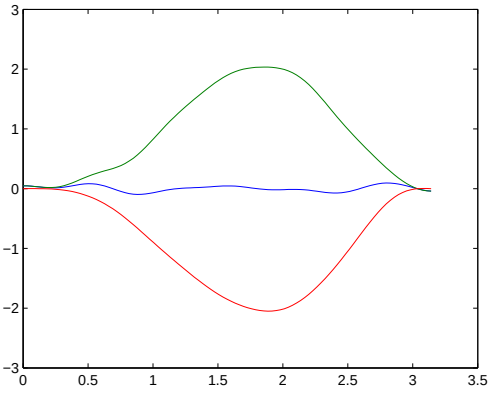

Figure 2b

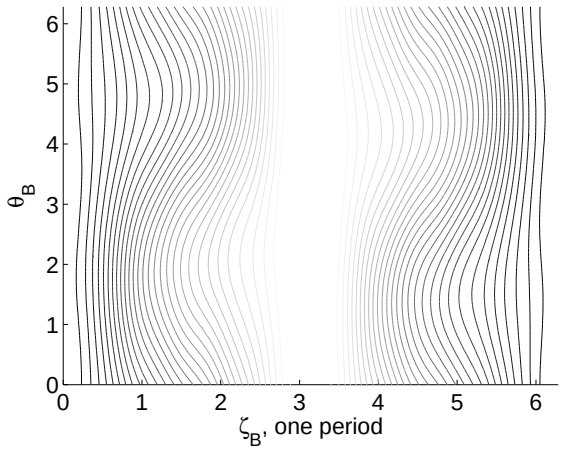

Figure 3

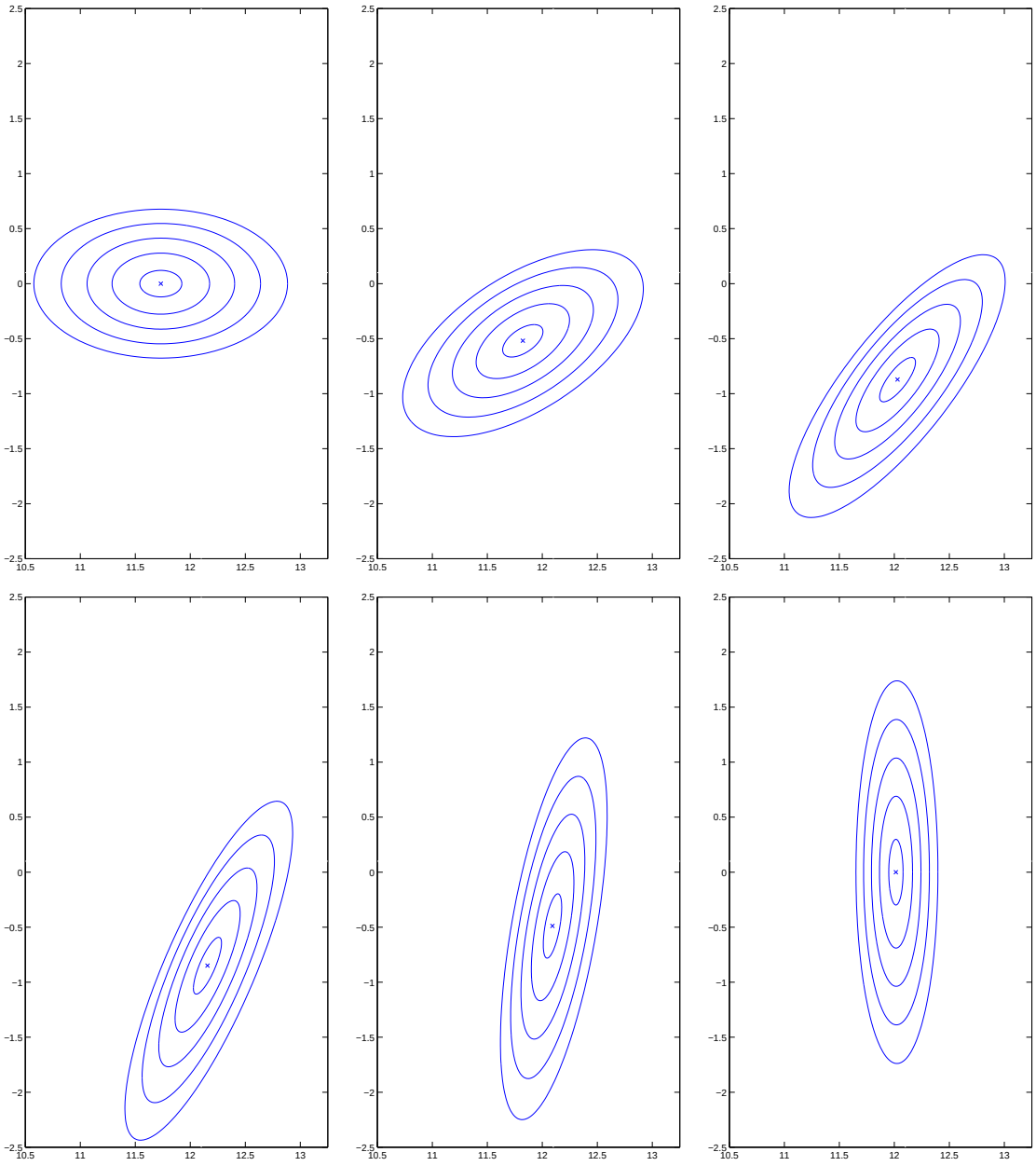

Figure 4

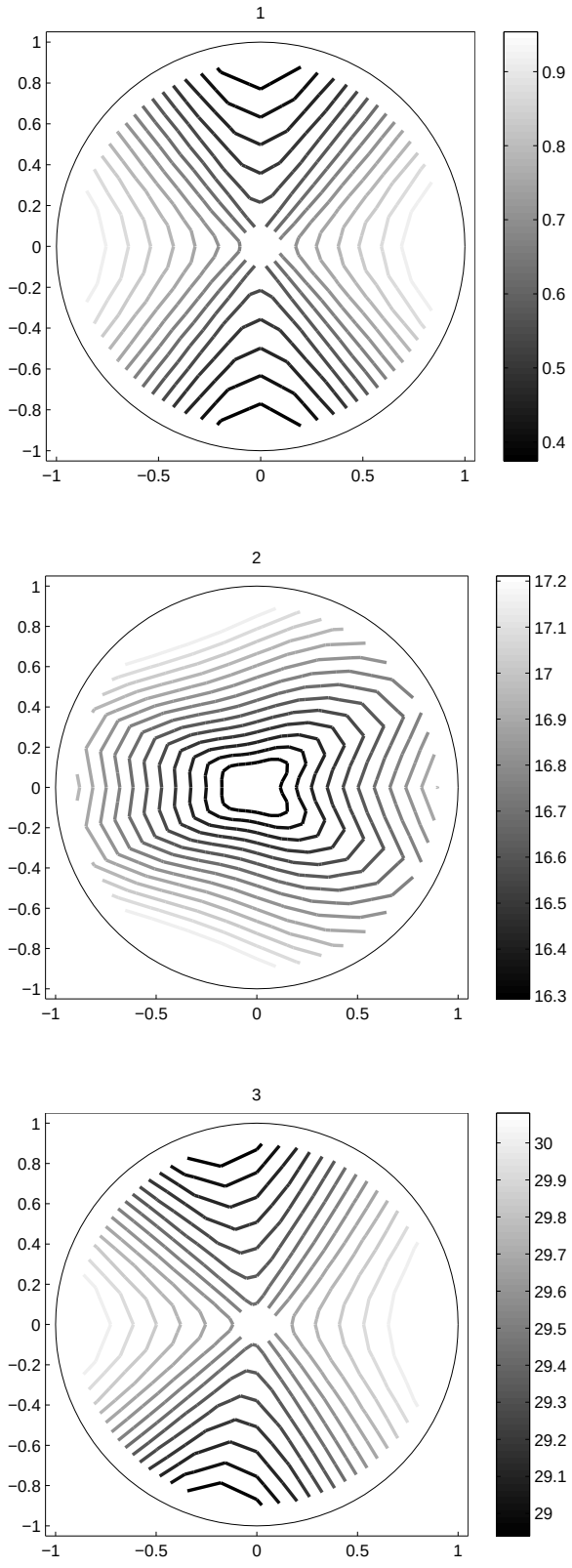
1
1
0.8
0.6
0.4
0.2
0
−0.2
−0.4
−0.6
−0.8
−1
−1
−0.5
0
0.5
1
0.9
0.8
0.7
0.6
0.5
0.4
2
17.2
17.1
17
16.9
16.8
16.7
16.6
16.5
16.4
16.3
3
30
29.9
29.8
29.7
29.6
29.5
29.4
29.3
29.2
29.1
29

Figure 5

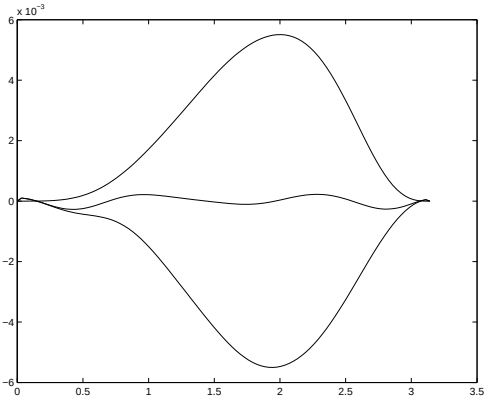

Figure 6